BRAIN CONNECTIVITY
Volume 5, Number 1, 2015

DOI: 10.1089/brain.2014.0230

Dynamic Repertoire of Intrinsic Brain States Is Reduced in Propofol-Induced Unconsciousness

Anthony G. Hudetz, Xiping Liu, and Siveshigan Pillay

Abstract

The richness of conscious experience is thought to scale with the size of the repertoire of causal brain states, and it may be diminished in anesthesia. We estimated the state repertoire from dynamic analysis of intrinsic functional brain networks in conscious sedated and unconscious anesthetized rats. Functional resonance images were obtained from 30-min whole-brain resting-state blood oxygen level-dependent (BOLD) signals at propofol infusion rates of 20 and 40 mg/kg/h, intravenously. Dynamic brain networks were defined at the voxel level by sliding window analysis of regional homogeneity (ReHo) or coincident threshold crossings (CTC) of the BOLD signal acquired in nine sagittal slices. The state repertoire was characterized by the temporal variance of the number of voxels with significant ReHo or positive CTC. From low to high propofol dose, the temporal variances of ReHo and CTC were reduced by 78% ± 20% and 76% ± 20%, respectively. Both baseline and propofol-induced reduction of CTC temporal variance increased from lateral to medial position. Group analysis showed a 20% reduction in the number of unique states at the higher propofol dose. Analysis of temporal variance in 12 anatomically defined regions of interest predicted that the largest changes occurred in visual cortex, parietal cortex, and caudate-putamen. The results suggest that the repertoire of large-scale brain states derived from the spatiotemporal dynamics of intrinsic networks is substantially reduced at an anesthetic dose associated with loss of consciousness.

Key words: consciousness; anesthesia; fMRI; functional connectivity; default mode network

Introduction

The quest for the neurobiological mechanisms of consciousness has been a supreme challenge for neuroscience and philosophy (Chalmers, 1998; Crick and Koch, 1998; Edelman et al., 2011; Seth et al., 2006; Tononi and Koch, 2008). Recently, a rapidly expanding group of investigators began to approach the problem by applying anesthetic agents to reversibly modulate the state of consciousness in search of unique neuronal correlates of state transitions in the brain in both humans and animals (Alkire et al., 2008; Boly et al., 2013; Bonhomme et al., 2012; Brown et al., 2010; Hudetz, 2012; Mashour and Alkire, 2013). Tentative findings have suggested a role for large-scale thalamocortical and corticocortical networks, subcortical modulatory and higher cortical integration centers in the orchestration of the reversible transitions between conscious and unconscious states (Alkire, 2008; Bonhomme et al., 2011; Boveroux et al., 2010; Ferrarelli et al., 2010; Guldenmund et al., 2013; Hudetz, 2012; Langsjo et al., 2012; Lee et al., 2009a, 2009b, 2013; Mhuircheartaigh et al., 2010; Nallasamy and Tsao, 2011; Peltier et al., 2005; Schrouff et al., 2011; White and Alkire, 2003). However, a final common pathway or unitary theory for losing and regaining consciousness has not emerged.

In most studies to date, functional networks of the brain have been mapped in steady states, confining their description to temporally enduring configurations, yielding an essentially binary distinction between neuronal networks that characterize the conscious versus the unconscious brain state (Bonhomme et al., 2012; Hudetz, 2012). More recently, it has been realized that brain networks undergo incessant spontaneous dynamic reconfigurations even in the absence of novel stimuli or cognitive task (Allen et al., 2012; Britz et al., 2010; Chang and Glover, 2010; Cribben et al., 2013; Di and Biswal, 2013; Glerean et al., 2012; Handwerker et al., 2012; Hutchison et al., 2013b; Jones et al., 2012; Kang et al., 2011; Keilholz et al., 2013; Liu and Duyn, 2013; Sakoglu et al., 2010; Tagliazucchi et al., 2012b). Such ''resting-state'' network dynamics has been ascribed to the general phenomena of spontaneous mentation, imagery, task-independent thoughts, or daydreaming (Mason et al., 2007). However, dynamic changes in brain connectivity have also been observed in anesthetized animals

Department of Anesthesiology, Medical College of Wisconsin, Milwaukee, Wisconsin.

(Hutchison et al., 2013b; Majeed et al., 2009) casting a doubt as to whether they are essential for conscious mentation.

A fundamental, heretofore unexplored question is how the diversity of dynamic configurations of resting-state brain networks may be altered during the transition to losing or regaining consciousness in the same subject. Is brain dynamics suppressed or augmented as the state of consciousness is altered and is it preferentially altered in specific brain networks? A current theory of consciousness postulates that the richness of conscious experience is related to the diversity or ''repertoire'' of causal states available to the brain (Tononi, 2004, 2012) and that anesthesia may suppress consciousness by shrinking this repertoire (Alkire et al., 2008). According to this hypothesis, either a reduction in the number of available states or a reduction in the frequency of their dynamic transitions could lead to a suppression of consciousness. To-date, the dynamic repertoire of brain states has not been quantified in different states of consciousness.

Motivated by these considerations, the goal of this investigation was to examine how a change in anesthetic depth producing loss of consciousness alters the dynamic repertoire of resting-state networks of the brain. We hypothesized that anesthetic-induced loss of consciousness will correlate with a substantial decrease in the diversity of states that the brain accesses over time. We devised a novel method to estimate the repertoire of states as the temporal variance of intrinsic networks derived from dynamic resting-state functional magnetic resonance imaging (fMRI) data. Imaging data were obtained in experimental animals because they were amenable to prolonged imaging scans in complete immobility required by the analysis. For anesthesia, we chose propofol, a common clinically used anesthetic agent that can be easily titrated to produce conscious sedated and unconscious states and has been frequently used in studies of human brain connectivity.

Materials and Methods

Animal preparation

Experimental procedures and protocols were approved by the Institutional Animal Care and Use Committee of the Medical College of Wisconsin (Milwaukee, WI). All procedures conformed to the Guiding Principles in the Care and Use of Animals of the American Physiologic Society and were in accordance with the Guide for the Care and Use of Laboratory Animals (National Academy Press, Washington, DC, 1996).

Six adult (250–350 g), male, Sprague-Dawley rats were kept in a reverse light–dark cycle room for at least 10 days prior to the experiment to minimize the effect of sleep pressure during the experiment. Food and water access was *ad libitum*. Aseptic technique was used during surgical preparation. Surgery was performed under 2% isoflurane anesthesia for placement of femoral lines for intravenous (iv) anesthetic delivery and arterial blood pressure monitoring, and tracheostomy for mechanical ventilation. Rats were then transferred to a G-10 fiberglass MRI cradle (Meditherm-III; Gaymar Industries, Orchard Park, NY) outfitted with water-recirculating heating system. Arterial blood pressure, heart rate, arterial oxygen saturation, core temperature, respiratory rate, inspired and expired oxygen and carbon-dioxide concentrations were continuously monitored during the experiment (POET IQ2 monitor; Criticare Systems, Inc., Waukesha, WI). After hemodynamic stabilization, the animals were weaned off the isoflurane and switched to propofol. The initial propofol infusion rate was either 20 or 40 mg/kg/h and reversed in consecutive experiments. These doses were chosen to produce conscious sedated and unconscious anesthetized states, respectively, based on prior studies of behavioral responses and electroencephalogram patterns in animals that did not receive muscle relaxant (Liu et al., 2013d). In the present study, propofol was added to pancuronium bromide (1 mg/kg/h, iv) and administered by a programmable MR-compatible infusion pump. The animals' lungs were artificially ventilated with 70/30 N_2/O_2 delivered at a flow rate of 5 L/min. Functional data were acquired after all physiological parameters were stable and within normal limits for at least 40 min.

Imaging

All fMRI data were acquired using a Bruker 9.4T AVANCE scanner, Bruker linear transmit coil (T10325), and rodent surface-receiving coil (T9208). High-resolution anatomical scans with relaxation enhancement rapid acquisitions (RARE) sequence, repetition time (TR) = 5000 msec, echo time (TE) = 11.3 msec, number of averages = 2, RARE factor = 8, field of view = 35×35 mm^2, matrix size of 256×256, slice thickness of 1 mm, and nine contiguous sagittal slices were obtained. Thirty-minute uninterrupted functional scans were acquired using a single-shot gradient echo-planar imaging sequence: TR = 1000 msec, TE = 19.5 msec, 1800 repetitions, matrix size = 96×96 with the same above geometry, x-y voxel size = 365×365 μm^2. Images were acquired in the sagittal plane to maximize the spatial resolution in the anterior–posterior direction. The nine sagittal slices provided nearly complete whole brain coverage with relatively few slices at 1 sec TR. The simultaneous maximization of temporal and spatial resolutions across the entire brain was considered essential for the estimation of the repertoire of global state configurations.

Each functional scan was repeated after switching to the other propofol dose following 10-min equilibration. After slice-timing and routine motion correction, the fMRI images were registered using the FLIRT program in FMRIB Software Library (FSL) (Jenkinson et al., 2002) onto the reference template from a select rat. Blood oxygen level-dependent (BOLD) signal time courses were detrended and low-pass filtered at 0.25 Hz (Magnuson et al., 2010; Majeed et al., 2009). Due to the use of muscle relaxant, head motion was negligible (less than two voxels in each spatial direction). For subsequent analysis, the first five points were discarded. The Analysis of Functional NeuroImages (AFNI) software package (NIH, Baltimore, MD) was used for fMRI data processing.

Brain states

Global brain states were defined as dynamic large-scale correlation patterns of BOLD signals in the resting state. To extract the resting-state networks dynamically, two methods of analysis were used: sliding-window regional homogeneity (ReHo), and coincident threshold crossing (CTC). To obtain ReHo, the 30-min fMRI scans were divided into consecutive sliding windows of 20, 50, 100, 200, and 400 sec with 90% overlap. The 200 sec windows with 90% overlap resulting in 81 sequential ReHo maps was used in the final analysis. ReHo was obtained as the Kendall's coefficient of

concordance to yield a nonparametric measure of similarity of each voxel's BOLD time series with those of its 27 nearest neighbors (Zang et al., 2004). The value of ReHo ranging from 0 to 1, and when calculated for all voxels across the brain, the resulting maps represent contiguous three-dimensional temporal correlation patterns. From all sliding windows, a common subset of voxels with ReHo values that exceeded the mean + 2 standard deviations (SDs) was found. To characterize the repertoire of states the brain accessed over the duration of each scan, the temporal variance of ReHo from these voxels across all sliding windows was calculated. K-mean clustering was used to select the most distinct ReHo patterns (maps) for visual display. The statistical distribution of temporal variance was calculated for each rat and compared between the two propofol doses.

The CTC method (as we call it) was applied to increase the temporal resolution even further. As recently introduced (Tagliazucchi et al., 2012a, 2012b), this method identifies patterns of spontaneous activity with the voxels whose BOLD signal momentarily crosses a predefined threshold - usually a certain multiple of SD for the same voxel. The analysis yields instantaneous maps of BOLD correlation patterns at the rate of the image acquisition, in our case TR = 1 sec, resulting in 1795 maps. To obtain (Tagliazucchi et al., 2012a) the CTC patterns of activity (CTC maps), we identified the voxels with BOLD signals that exceeded 1, 2, 3, or 4 SDs in each rat, at each propofol dose. The mean BOLD signal within each image slice or across the whole brain was previously subtracted from all BOLD time courses. For display, the images were compressed by the inverse Fisher's Z transform. The number of voxels that crossed threshold and the average BOLD signal in the same voxels were calculated at 1795 time points at 1 sec increments. The temporal variance of the average BOLD exceeding threshold was calculated as a measure of the dynamic state repertoire for the duration of each scan. The frequency distribution of distinct activity patterns was determined by hierarchical clustering into 90 types. All pair-wise distance of maps was obtained using Spearman's rank correlation followed by the calculation of weighted average distance among the clusters. In each rat, temporal variance was calculated for the whole brain, and for individual image slices and compared between two propofol doses.

For group analysis, the BOLD time courses from all rats and both doses were concatenated to yield a string of 21540 BOLD images and CTC maps. Hierarchical clustering was then applied to all maps. The number of unique maps and the temporal variance of the average BOLD signal for voxels that crossed threshold were determined separately for the low dose and high dose segments of the data. To estimate the temporal variance in specific brain regions, 12 regions of interest (ROIs) were manually defined based on sagittal sections of the Paxinos rat brain atlas (Paxinos and Watson, 2007). The following cortical ROIs were delineated: anterior cingulate (AC), primary motor (M1), primary sometosensory (S1), parietal association (PtA), primary and secondary visual (V1/V2), and retrosplenial cortex (Retro). Subcortical ROIs were as follows: hippocampus (Hipp), caudate-putamen (CPu), nucleus basalis of Meynert (NBM), medial thalamus (mTh), hypothalamus (Hypo), and nucleus pontis oralis (PnO). The ROIs were chosen to cover the most extensive cortical regions and important subcortical centers suggested to be involved in the anesthetic modulation of the ascending arousal system (Alkire et al., 2007; Brown et al., 2010; Devor and Zalkind, 2001; Guldenmund et al., 2013; Mhuircheartaigh et al., 2010; Sukhotinsky et al., 2007; Zecharia and Franks, 2009). Group analysis for 12 ROIs involved the calculation of CTC temporal variance at each propofol dose and the relative contribution of each ROI to the dose-dependent change in global variance. The latter quantity was calculated by weighting the variance in each ROI by the number of voxels contained and normalizing as (VL-VH)*NV/TNV/VLH, where VH and VL are the variances in an ROI at the low and high doses, respectively, NV is the number of voxels in the respective ROI, TNV is the total number of voxels in all ROIs, and VLH is the average of VL-VH across all ROIs. All calculations were done using Matlab 7.3 (Mathworks, Inc., South Natick, MA).

Statistics

Using data from the first three animals, we calculated effect size (Cohen's *D*) and rat number required to achieve statistical power of 80% as a function of sliding window length. From the calculated ReHo temporal variance at two propofol levels, effect size decreased at shorter window lengths as follows: 1.6 (400 sec), 1.66 (200 sec), 0.97 (100 sec), 0.87 (50 sec), and 0.75 (20 sec). With the effect size for 400 and 200 sec windows, $n = 6$ was found to be adequate. For shorter windows (effect size < 1.0) the required number of animals needed would have been 14 or more. To achieve optimal temporal resolution at six animals we chose 200 sec for further analyses.

The effect of propofol dose on the temporal variance of ReHo or BOLD signal above threshold (CTC method) was tested using repeated measures ANOVA with rat as subject and dose as within factor. In case of the CTC data, the image slice and SD factor were used as additional independent variables. *Post hoc* tests of the propofol dose effect were conducted at individual SD factors for the three middle slices combined. Statistical tests were performed using the software NCSS 2007 (NCSS, Kaysville, UT).

Results

Physiology

The animals' systemic physiological variables were stable throughout the course of the experiment. Mean arterial blood pressure, heart rate, peripheral arterial oxygen saturation, and core body temperature were within the normal physiological range at both anesthetic levels (Table 1). There was no indication of distress, for example, a sudden increase in heart rate or blood pressure, at either dose of the anesthetic. All animals completed the entire experimental protocol.

Table 1. Physiological Variables

Propofol dose (mg/kg/h)	*BP (mmHg)*	*HR (bpm)*	*SPO_2 (%)*	*T (°C)*
20	149 ± 18	323 ± 16	96 ± 3	37.4 ± 0.3
40	142 ± 21	327 ± 20	94 ± 5	37.7 ± 0.2

Mean ± standard deviation.
BP, mean arterial blood pressure; HR, heart rate; SPO_2, saturation of peripheral oxygen; T, temperature.

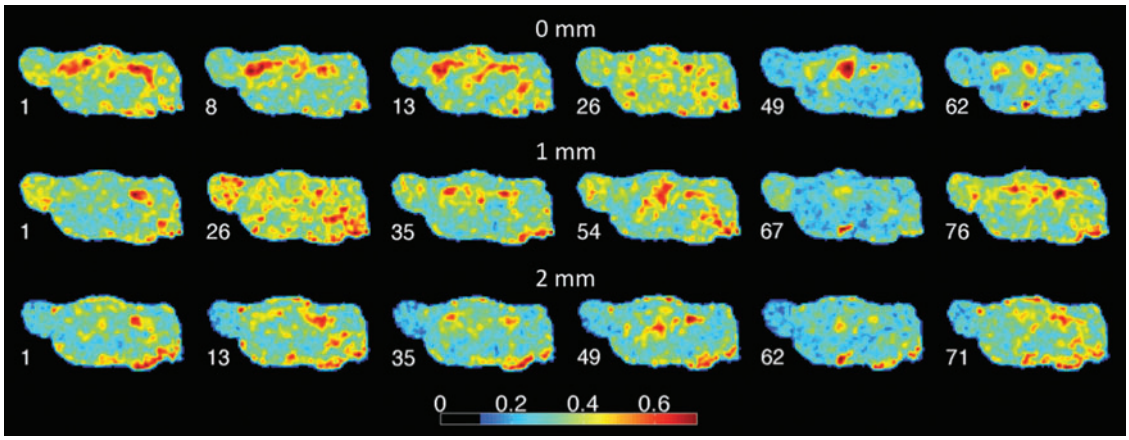

FIG. 1. Dynamic analysis of regional homogeneity (ReHo). Snapshots of ReHo patterns are shown in one rat in three sagittal slices at 2, 1, and 0 mm from midline. Numbers above the images indicate the time (sec) of the image taken from a 30 min scan. Color code shows ReHo value.

Regional homogeneity

Dynamic brain states were first characterized by an extraction and enumeration of resting-state connectivity using the ReHo method. As mentioned before, ReHo reflects close-range spatial clustering of BOLD hotspots. Figure 1 shows snapshots of typical ReHo maps during select time intervals in one animal. The six maps were chosen using K-means clustering to illustrate those that are most distinct from each other. The variability in ReHo patterns is presumed to be essential for the temporal diversity of brain states.

The effect of anesthetic dose on the state repertoire was then quantified by the temporal variance of significant ReHo values across the 81 sliding windows of 200 sec length each. Figure 2 shows the frequency distribution of ReHo temporal variance at the two conditions in six experiments. It is clear that in every case, the variance was substantially reduced at the higher propofol dose. The average decrease

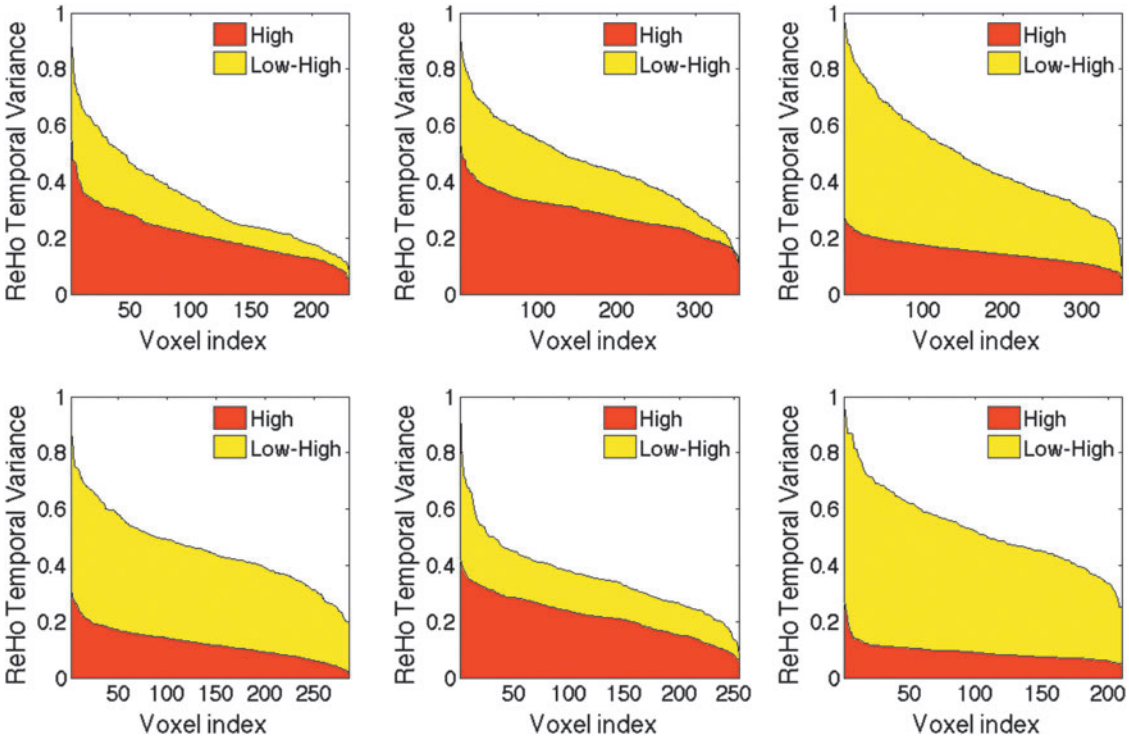

FIG. 2. Voxel-wise distribution of ReHo temporal variances in six rats at two doses of propofol. Variance values are sorted in descending order and plotted against the voxel index. Area in red color shows ReHo variance distribution at the high dose; yellow area corresponds to the difference between low dose and high dose. ReHo temporal variance values are reduced by 45–142% at the high dose in various animals.

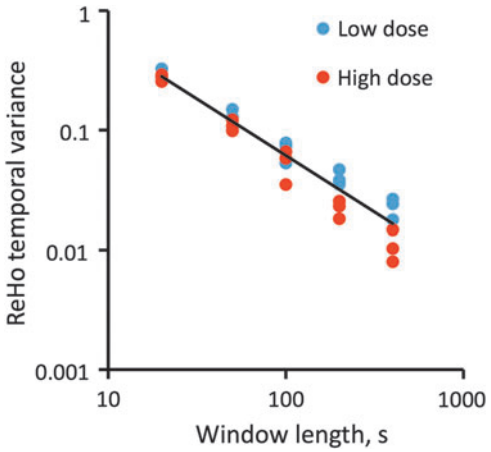

FIG. 3. Temporal variance of ReHo decreases exponentially as a function of sliding window length. The difference between low and high propofol doses increases with longer windows.

in temporal variance from all experiments was 78% ± 20% ($p < 0.05$), suggesting a dramatic reduction in the state repertoire in the unconscious condition.

We also investigated the effect of sliding window length between 20 and 400 sec on the results. As Figure 3 illustrates, with shorter windows, the ReHo temporal variance increased and the effect of propofol dose was diminished (~6% at 20 sec). The overall dependence of ReHo temporal variance on window length followed an exponential function (linear fit on log-log plot, $R^2 = 0.999$). At 200 and 400 sec window lengths a substantial dose effect was seen that was significant at 80% power, $n = 6$. Given that a shorter window allows better temporal resolution, the 200 sec window length appeared an optimal choice for the analysis.

To verify that the effect of anesthesia was not due to a reduction in random noise in the system, we recalculated the temporal variance after randomizing the BOLD signal time series in each voxel. The variance after randomization dropped to 11% of its original value (at the lower dose) and was unaffected by the higher anesthetic dose. This result confirmed that the fluctuations in ReHo were in fact functional and not due to random noise.

Because brain states were defined by the spatial patterns of correlated activity, the repertoire of states could also depend on the degree of connectivity. We calculated the average cross-correlation coefficients within the significant ReHo regions and found that they were similar in the two anesthetic conditions: 0.50 ± 0.15 (low dose) and 0.54 ± 0.19 (high dose). This suggested that the principal target of anesthesia was not the degree of regional connectivity, but the temporal dynamics of network states.

Coincident threshold crossing

The dynamic repertoire of brain states was also analyzed from correlated BOLD activity based on coincident BOLD threshold crossings that gives a high temporal resolution of 1 TR or in this case, 1 sec. Figure 4 shows snapshots of CTC maps, highlighting those most frequently recurring as identified by the method of hierarchical clustering in three rats. The dynamics of brain states was quantified by the number of voxels crossing threshold in each map as a function of time. Figure 5 illustrates the dynamic fluctuation in the average BOLD over 1 SD threshold at two anesthetic conditions. A large reduction in the dynamics at the higher anesthetic dose is evident. To estimate the effect of anesthetic dose on the dynamic state repertoire, the temporal variance of all CTC voxels in the whole brain was calculated in each experiment. We obtained a 76% ± 20% ($p < 0.001$) reduction at the higher dose, again suggesting a substantial reduction in the repertoire of distinct brain states.

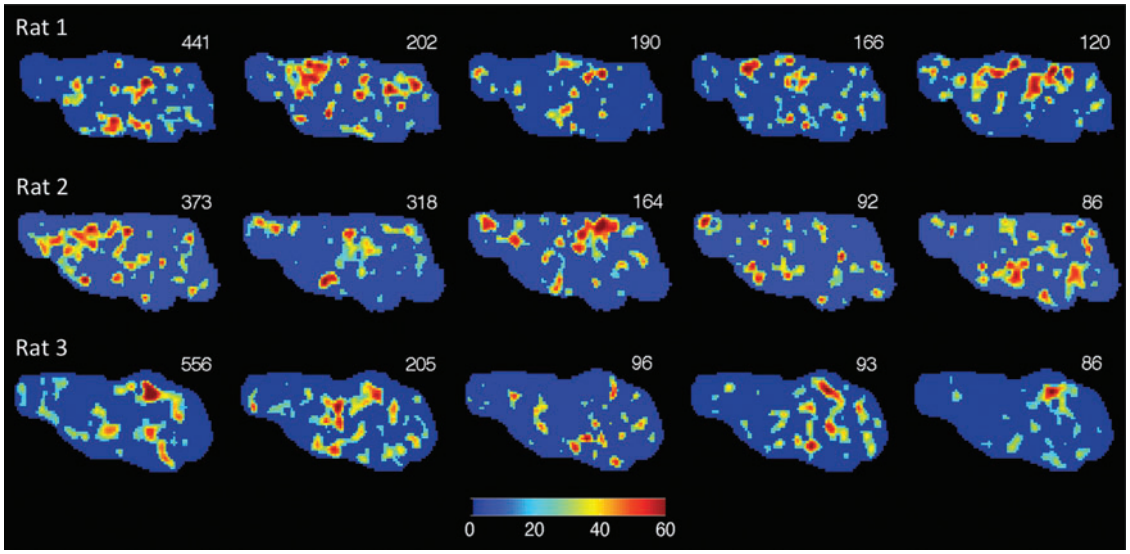

FIG. 4. Analysis of the dynamic repertoire of blood oxygen level-dependent (BOLD) fluctuation patterns using the coincident threshold crossing (CTC) method. The most frequently occurring CTC patterns as identified by hierarchical clustering into 90 types are shown. The count of each pattern from a total of 1795 patterns is indicated in the upper right corner of each image. Images in each row are from a different rat; all images are from the sagittal slice at midline.

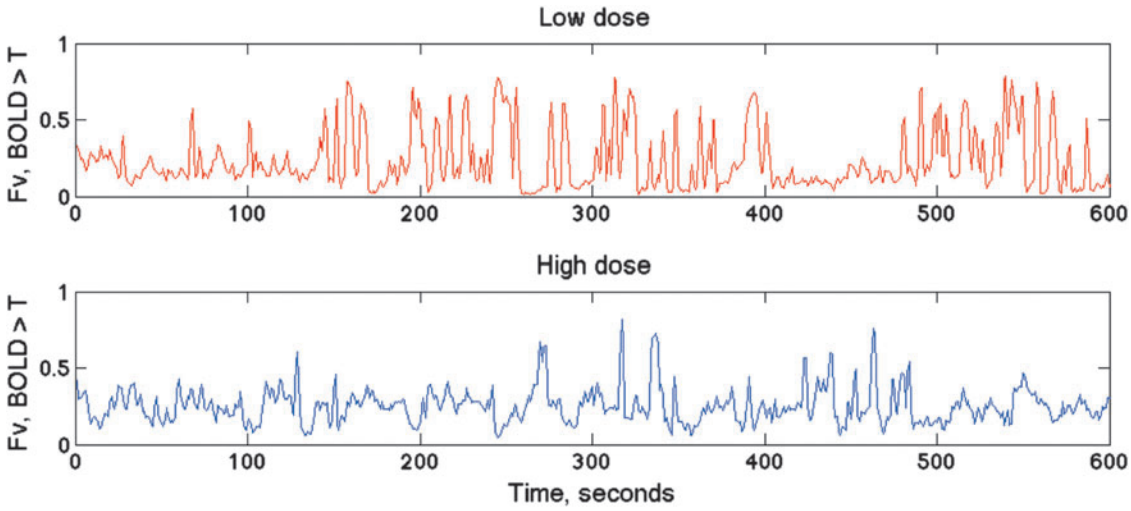

FIG. 5. Time course of average BOLD signal above one standard deviation (SD) threshold in one rat. The fluctuations are reduced at the higher propofol dose.

With the CTC method, we were also able to examine the temporal variance in each individual image slice. Figure 6 reveals that the temporal variance of the number of voxels crossing threshold gradually increased in consecutive slices in the lateral to medial direction. This was true with various chosen thresholds used to determine zero crossings of the BOLD signal. Moreover, the relative change in the temporal variance also increased in the lateral to medial direction at all thresholds. The maximum change in CTC variance in the three middle slices was $72\% \pm 18\%$ ($p < 0.001$) at a threshold of 4 SD. The dependence of CTC temporal variance on SD threshold in the three slices closest to the midline is illustrated in Figure 7. The observed difference was significant at all SD values ($p < 0.001$).

Group analysis of all CTC data revealed similar changes to those from individual rats. First, we found that the number of unique states (BOLD threshold crossing patterns) decreased by 20%, from 81 (low dose) to 66 (high dose) as obtained by hierarchical clustering of the zero-crossing BOLD patterns into 90 types. Second, by calculating the temporal variance of BOLD values crossing threshold in 12 individual ROIs, substantial decreases ranging from 38% to 77% were observed at the higher propofol dose (Fig. 8A). The contribution of each ROI to the change in global variance was estimated by weighting the variance change with the number of voxels in each ROI. As seen in Figure 8B, the relative contribution of ROIs was the highest in visual and parietal cortex and in caudate putamen. Smaller changes were seen in

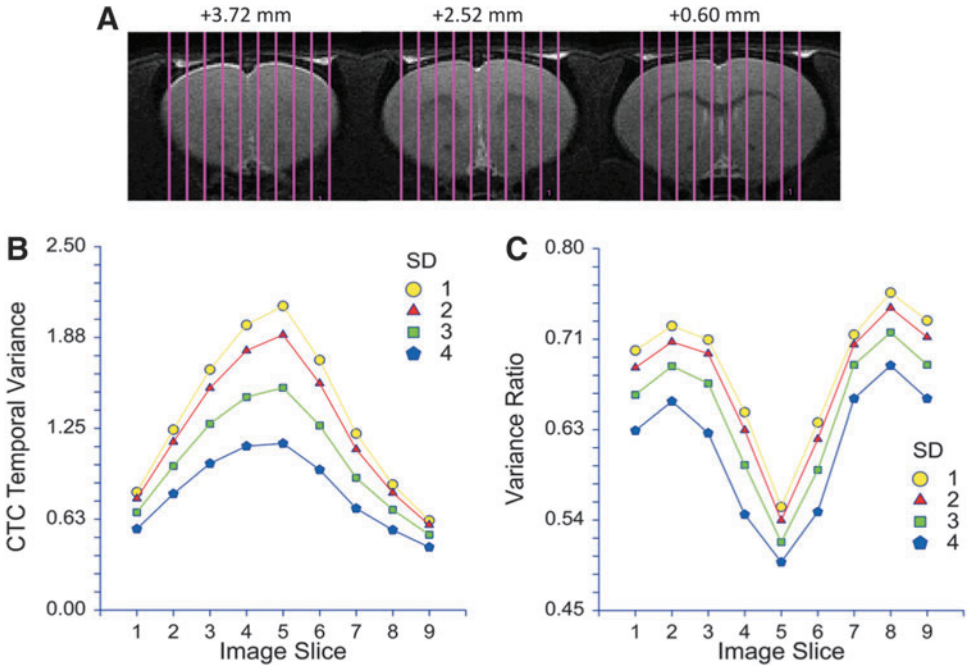

FIG. 6. Temporal variance of CTC patterns as a function of mediolateral position and SD threshold used to determine the zero crossings of the BOLD signal. **(A)** Brain coverage by the nine sagittal image slices at three frontocaudal positions from Bregma as indicated. **(B)** The temporal variance in the wakeful state is the largest near the midline (image slice 5) and is generally lower with the higher SD threshold. **(C)** Ratio of variances at high and low propofol dose increases toward the brain's midline at all SD thresholds. The drop in variance ratio in slices 1 and 9 is likely related to an edge effect due to curvature of the brain's surface.

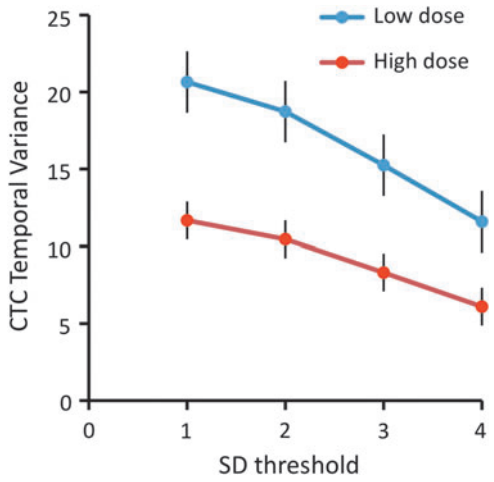

FIG. 7. Temporal variance of the BOLD signal at four different SD thresholds in the three slices closest to the brain's midline. The higher propofol dose significantly reduces temporal variance at all thresholds 1–4 SD.

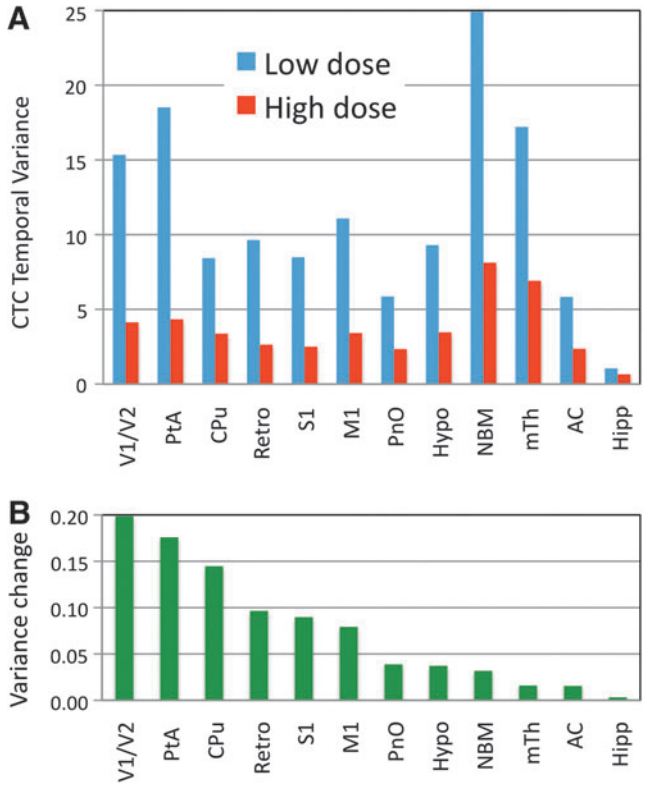

FIG. 8. Results of CTC group analysis for individual regions of interest (ROIs). **(A)** Average temporal variance for voxels with BOLD signal above 1 SD threshold within each ROI at low and high propofol doses. **(B)** Relative contribution of each ROI to the change in temporal variance between the low and high propofol doses. The change in variance weighted by the number of voxels contained by each ROI. See main text for an explanation of ROI abbreviations.

somatosensory, motor, and retrosplenial cortices. The contribution from subcortical structures was relatively low, in part due to the smaller number of voxels contained in most of these ROIs. When data from the 12 ROIs were combined, the average change in CTC variance was $64\% \pm 10\%$, quite consistent with the result from whole-brain analysis.

Discussion

In the present work we examined, from time-resolved resting-state whole-brain BOLD fMRI data, the temporal variance of brain networks, and found a substantial reduction in the dynamic repertoire of brain states during propofol anesthesia. This finding is novel in that the dose-dependent effect of anesthesia on the dynamics of brain states has not been demonstrated to date. The observed reduction in the dynamic repertoire of brain states supports the information integration theory of consciousness.

In most neuroscientific accounts, consciousness is thought to be an emergent property of complex brain networks (Crick and Koch, 1998; John, 2001; Mashour and Alkire, 2013; Tononi, 2012). The information integration theory of consciousness (Tononi, 2012) postulates that consciousness is equivalent to integrated information in the brain. Moreover, the level of consciousness depends on both the amount of information and its levels of integration. Based on this theory, we proposed (Alkire et al., 2008) that anesthetics may suppress consciousness by blocking the brain's ability to integrate information either by interrupting neuronal communication (causing a loss of integration) or by reducing the repertoire of distinct brain states (causing a loss of information). In practical terms, anesthesia may reduce the overall strength of brain connectivity, fragment neuronal networks, or decrease the repertoire of brain states by reducing those to stereotypic forms. Any of these changes would lead to a decrease in integrated information. It follows from the theory that consciousness should form a continuum; from fully alert wakefulness to complete oblivion, with possibly no distinct transition of state in the brain. Nevertheless, other theories suggest that loss of consciousness in anesthesia is associated with a distinct global state transition at a critical dose (Steyn-Ross et al., 2004). From a clinical point of view, a binary transition from conscious to unconscious state appears plausible. Whether consciousness is lost in a graded manner or all-or-none manner has been a matter of debate (Hudetz, 2008; Veselis, 2001). A plausible resolution to this apparent conflict has been provided by Sanders and coworkers (2012) who suggested that unconsciousness and unresponsiveness are distinguishable qualities of state.

In this work, propofol was administered at infusion rates chosen to produce clinically defined conscious sedated and unconscious anesthetized states. We chose to compare the unconscious condition to sedated condition instead of wakeful (drug free) condition for several reasons. First, functional imaging of sedated as opposed to awake animals avoids undue stress from the necessary immobilization and background noise that otherwise could produce confounding changes in brain activity and dynamics not uniquely associated with the state of consciousness itself. Second, reducing the difference in anesthetic dose between the conscious and unconscious conditions (as defined clinically) helps reduce the chance for nonspecific drug effects (Langsjo et al., 2012) that may cause additional changes in brain dynamics not associated with the state of consciousness *per se*.

The two anesthetic conditions used here were previously validated to satisfy behavioral and electrophysiological criteria to study the transition between sedation and anesthesia as observed in nonparalyzed animals using a behavioral response battery (Jugovac et al., 2006; Liu et al., 2013d). At the low propofol dose, the animals were generally immobile and docile, but remained responsive to various sensory stimuli. At the high propofol dose, the same rats lost their righting reflex—a putative index of conscious state (Franks, 2008), and no longer responded to non-noxious sensory stimulation. Consistent with the behavioral assessment, the frontal EEG changed from desynchronized pattern at the low dose to synchronized, slow wave pattern at the high dose as indicated by an increase in delta and theta band powers, and a decrease in 30–140 Hz gamma band power (Liu et al., 2013d). These observations strongly suggest that the rats were clinically conscious at the low but unconscious at the high propofol dose. Thus, the observed reduction in the brain's state repertoire may represent the critical stage of lost overt responsiveness along the graded effect of anesthesia on brain dynamics and consciousness.

Previous studies demonstrated diverse effects of anesthesia on resting-state brain connectivity (Boly et al., 2013; Bonhomme et al., 2011, 2012; Hudetz, 2012; Nallasamy and Tsao, 2011). The early work of Kiviniemi and associates (2005) indicated that sedative levels of the intravenous anesthetic, midazolam enhanced the amplitude and synchrony of spontaneous BOLD signal fluctuations. Greicius and coworkers (2008) found a general preservation of default mode connectivity with specific focal reductions in the posterior cingulate cortex that were different from the patterns seen with the volatile anesthetic, sevoflurane (Peltier et al., 2005). During sedation with propofol, regionally diverse, dose-dependent changes in resting-state connectivity have been found (Hudetz, 2012; Liu et al., 2013d). In particular, a breakdown of functional or effective connectivity has been demonstrated with both fMRI and electrophysiological methods (Boveroux et al., 2010; Ferrarelli et al., 2010; Gomez et al., 2013; Lee et al., 2009a; Liu et al., 2012; Schrouff et al., 2011). Functional connectivity changes in both thalamocortical (Alkire et al., 2000; Liu et al., 2013c; White and Alkire, 2003) and corticocortical networks (Alkire and Miller, 2005; Boly et al., 2012; Boveroux et al., 2010; Ferrarelli et al., 2010; Hudetz, 2012; Schrouff et al., 2011; Soddu et al., 2012) have been detected. A reduction in the coherence and information transfer among select frontal, parietal, and occipital cortical regions has been found using electrophysiological techniques (Ku et al., 2011; Lee et al., 2009b, 2013). More generally, anesthetics have been thought to target subcortical mechanisms (Brown et al., 2010; Guldenmund et al., 2013; Mhuircheartaigh et al., 2010) including the natural sleep promoting circuits (Franks and Zecharia, 2011; Zecharia and Franks, 2009), and the neocortex itself (Hentschke et al., 2005; Hudetz, 2006; Seth et al., 2005; Velly et al., 2007).

Several fMRI studies have demonstrated resting-state brain networks in awake and anesthetized rodents (Becerra et al., 2011; Hutchison et al., 2010; Kalthoff et al., 2011; Liang et al., 2011; Liu et al., 2011; Lu et al., 2012; Nasrallah et al., 2012; Pawela et al., 2008; Tu et al., 2011; Upadhyay et al., 2011; Wang et al., 2011; Williams et al., 2010; Zhang et al., 2010; Zhao et al., 2008). However, only a few investigators have examined dynamic connectivity in anesthetized rodents (Keilholz et al., 2013; Magnuson et al., 2010; Majeed et al., 2009) or primates (Hutchison et al., 2013b; Liu et al., 2013a; Vincent et al., 2007). Dose-dependent comparisons across anesthetic levels relevant for the loss of consciousness in rodents have been particularly scarce (Liu et al., 2013d; Tu et al., 2011; Wang et al., 2011).

To quantify the dynamic repertoire of brain states, we used two different methods for mapping resting-state brain connectivity patterns and arrived at similar and robust changes in the repertoire as a function of the anesthetic dose. Global brain states were represented by the large-scale correlation patterns of BOLD signals corresponding to resting-state networks extracted dynamically, using either ReHo or CTC. Both of these methods are ''model-free'' in that they do not require *a priori* selection of ROI or ''seeds'' of correlation, and both are suitable to the dynamic representation of states that the brain accesses over time. ReHo is a measure of the short-range spatial correlation of BOLD activity (Liu et al., 2010; Zang et al., 2004) reflecting the tendency of neural activity to spatially cluster around regional hotspots. Thus, voxels with high ReHo values delineate multiple contiguous regions of correlated BOLD fluctuations. Here, we applied the ReHo method to a dynamic analysis of correlated brain activity for the first time. The CTC method (as we call it) was designed to quantify spontaneous spatiotemporal correlation patterns at high temporal resolution representing the BOLD signal as a point process (Tagliazucchi et al., 2011). The method has been shown to yield networks that are consistent with those obtained by independent component analysis (ICA) on a longer time scale and has been shown to track changes in state of vigilance (Tagliazucchi et al., 2012b).

Alternative approaches to delineate large-scale intrinsic networks of the brain include sliding window ICA (Kiviniemi et al., 2011), temporal ICA (Smith et al., 2012), and others (Cribben et al., 2013) [for a comprehensive review see Hutchison et al. (2013a)]. In a recent analysis of dynamic resting-state connectivity, Allen and colleagues (2014) applied group-level spatial ICA to decompose data from 405 subjects into 50 components as intrinsic networks and then characterized the dynamics by tapered sliding-window correlation matrices of these components. They then used k-means clustering to identify recurring, quasi-stable patterns as ''functional connectivity states'' and describe their variability and transition dynamics. Our definition of brain states was different; instead of the all pair-wise correlation matrix of entire networks, our states were based on voxel-wise correlation within a subset of the whole brain as defined by either ReHo or CTC. Also, the resting-state scans in Allen's study were relatively short (5 min), and only seven connectivity states common to all subjects were delineated. In any case, the dynamic variability of connectivity states, albeit defined differently, was substantiated by both studies.

Liu and associates (Liu and Duyn, 2013; Liu et al., 2013b) applied a variation of the point process method (Tagliazucchi et al., 2011) followed by k-means clustering in terms of the spatial similarity of BOLD signal activations or deactivations to derive spontaneous coactivation patterns (CAPs). In Liu and colleagues (2013b), they admitted 10% of the highest and 5% of the lowest signal values (after demeaning and normalizing to temporal SD) and averaged the signal patterns obtained at various time points within each cluster. Because each CAP represented an average from many time points and

the CAPs were relatively few, they did not lend themselves to an analysis of temporal variability. In our analysis, all time points that crossed threshold were included and used to calculate the temporal variance of the spatially averaged, suprathreshold BOLD signal. K-means clustering was used to illustrate the spatial distribution and frequency of recurrence of the CTC patterns but did not enter the calculation of temporal variance.

Recently, Di and Biswal (2013) employed a combination of group ICA and point process analysis to examine dynamic variations in resting-state functional connectivity as a function of intrinsic activities of specific networks and they found network-specific associations between the two. They examined both positive and negative threshold crossings (peaks and throughs) of the BOLD signal and used those to delineate regions with dynamically high and low activity, respectively. We focused on the dynamics of peaks alone because of their presumed relationship with increased neuronal activity. Nevertheless, in a few instances, we also calculated the CTC temporal variance from negative threshold crossings (troughs). The effect of propofol dose on temporal variance of troughs was similar to that reported for the peaks although it was less consistent among the animals. We tentatively concluded that the anesthetic effect on brain states was correlated more closely with the dynamics of spontaneous activations than the dynamics of spontaneous deactivations.

Why do the peak threshold crossings diminish in anesthesia? It has been shown that after the induction propofol anesthesia, the ongoing neuronal activity becomes spatiotemporally fragmented (Lewis et al., 2012), presumably resulting in fewer activation events that account for the BOLD threshold crossings. Also, as we have seen, neuronal activation patterns become more stereotypical, entailing a reduced variance in the size and pattern of spontaneous BOLD activations. Both of these changes may reduce the diversity of functional configurations, that is, the state repertoire, as we have found here.

The use of temporal variance to estimate the repertoire of brain states is a novel aspect of this work. While this is an intuitive idea, there may be other measures that satisfy the task of enumerating the diversity of brain states. Calculating the rate of change of network configurations may be a plausible alternative. Various entropy-based measures have also been employed to characterize the distribution and complexity of neuronal systems. Most approaches of this sort describe stationary properties of a system as opposed to their dynamic evolution with a notable exception (Balduzzi and Tononi, 2008). A novel entropy-based index of consciousness, the perturbational complexity index (PCI), which reliably discriminates the levels of human consciousness among wakefulness, sleep, and anesthesia was recently developed (Casali et al., 2013). Assessment of the PCI involves transcranial magnetic stimulation that was not performed in our present study. However, it may be relatively straightforward to design experiments with cortical stimulation to test the performance of PCI in our animal model in the future.

An outstanding question relates to the spatiotemporal organization at which the repertoire of brain states should be measured. It is plausible that the organizational complexity and the number of distinct functional states of the brain would be higher when measured at finer spatial and temporal scales. However, the level of organization at which conscious experience is instantiated is not yet clear. It may span several hierarchical levels from synapses, neurons, and local circuits, to regions and networks, and so estimating the state repertoire at the fMRI voxel level is only one possibility. Nevertheless, from the point of view of consciousness and its modulation by anesthetics, large-scale integration in the brain appears to be an essential feature to account for, at any spatiotemporal resolution. While the spatiotemporal resolution of fMRI is relatively coarse, the number of combinatorially possible network patterns defined at voxel level is enormous, and prolonged fMRI scans give us a fairly large sample of possible state configurations. In addition, fMRI provides a unique opportunity to examine the effect of anesthetics on information integration in the whole brain. Complementary investigations at the level of cellular or subcellular organization may provide refined measures in the future if and when corresponding dynamic measurements will be simultaneously performed across the entire brain.

As in all pharmacological fMRI investigations, the potential influence of physiological and hemodynamic factors should be taken into account (Biswal and Kannurpatti, 2009; Kannurpatti et al., 2003a). The effects propofol on mean arterial pressure and global cerebral blood flow are relatively small (Fiset et al., 2005; Liu et al., 2013d). Therefore, pressure-dependent changes in low-frequency hemodynamic fluctuations (Biswal and Kannurpatti, 2009) in the present study were unlikely. One could raise the possibility that propofol could still influence network connectivity by altering neurovascular coupling (Liu et al., 2013a; Masamoto and Kanno, 2012). However, given the preservation of functional responses during propofol anesthesia (Franceschini et al., 2010), resting-state connectivity most likely reflected underlying fluctuations in neuronal connectivity. Arterial CO_2 is another important physiological variable that may significantly influence low-frequency BOLD fluctuations and functional connectivity (Biswal et al., 1997; Hudetz et al., 1992, 1995; Kannurpatti et al., 2003b). Although arterial blood samples were not taken in this study, P_aCO_2 values measured in parallel experiments at the same propofol doses used here were found within normal limits (Liu et al., 2013d).

Finally, in this work, we examined the anesthetic effect without *a priori* assumptions for the anesthetics' regional targets. Nevertheless, when analyzing the dynamic correlated activity at high temporal resolution, the dynamic repertoire showed increasing sensitivity to anesthetic modulation in the lateral to medial direction. The network encompassing the anterior and posterior cingulate, retrosplenium and precuneus, all adjacent to the brain's midline, has been identified in humans as the ''default mode'' network (Raichle et al., 2001) that is predominantly active in task-free conditions engaging in self-directed mental activity (Gusnard et al., 2001). The default network has been recently identified in rodents as well (Lu et al., 2012; Upadhyay et al., 2011; Zhang et al., 2010). Given the putative role of this network in internal awareness (Sanders et al., 2012), our finding that in the conscious condition, the temporal variance was the highest in this region and it was the most reduced in the unconscious condition is interesting. The ROI-based analysis of temporal variance changes with the anesthetic level confirmed the involvement of the default mode network (DMN) components although the largest changes in variance occurred in visual

and parietal cortices and in the caudate-putamen. The latter is interesting as the functional connectivity of the putamen with other brain regions was quite sensitive to modulation by propofol anesthesia (Mhuircheartaigh et al., 2010). Further ROI-based analyses would require a larger sample size but will be of interest to more precisely delineate the involvement of DMN and other intrinsic networks in dynamic connectivity changes with anesthesia in the future. In any case, the reduction in large-scale dynamic repertoire at the critical anesthetic dose appears to correlate with the suppression of consciousness in the context of the information integration theory of consciousness.

Acknowledgments

The authors express their gratitude to Dr. Giulio Tononi, University of Wisconsin—Madison and two anonymous reviewers for their insightful comments that helped improve the final article. Research reported in this publication was supported by the National Institute of General Medical Sciences of the National Institutes of Health under Award Number R01-GM056398 and by the National Institute of Biomedical Imaging and Bioengineering of the National Institutes of Health under Award Number R01-EB000215. The content is solely the responsibility of the authors and does not necessarily represent the official views of the National Institutes of Health.

Author Disclosure Statement

No competing financial interests exist.

References

Alkire MT. 2008. Loss of effective connectivity during general anesthesia. Int Anesthesiol Clin 46:55–73.

Alkire MT, Haier RJ, Fallon JH. 2000. Toward a unified theory of narcosis: brain imaging evidence for a thalamocortical switch as the neurophysiologic basis of anesthetic-induced unconsciousness. Conscious Cogn 9:370–386.

Alkire MT, Hudetz AG, Tononi G. 2008. Consciousness and anesthesia. Science 322:876–880.

Alkire MT, McReynolds JR, Hahn EL, Trivedi AN. 2007. Thalamic microinjection of nicotine reverses sevoflurane-induced loss of righting reflex in the rat. Anesthesiology 107:264–272.

Alkire MT, Miller J. 2005. General anesthesia and the neural correlates of consciousness. Prog Brain Res 150:229–244.

Allen EA, Damaraju E, Plis SM, Erhardt EB, Eichele T, Calhoun VD. 2014. Tracking whole-brain connectivity dynamics in the resting state. Cereb Cortex 24:663–676.

Balduzzi D, Tononi G. 2008. Integrated information in discrete dynamical systems: motivation and theoretical framework. PLoS Comput Biol 4:e1000091.

Becerra L, Pendse G, Chang PC, Bishop J, Borsook D. 2011. Robust reproducible resting state networks in the awake rodent brain. PLoS One 6:e25701.

Biswal B, Hudetz AG, Yetkin FZ, Haughton VM, Hyde JS. 1997. Hypercapnia reversibly suppresses low-frequency fluctuations in the human motor cortex during rest using echo-planar MRI. J Cereb Blood Flow Metab 17:301–308.

Biswal BB, Kannurpatti SS. 2009. Resting-state functional connectivity in animal models: modulations by exsanguination. Methods Mol Biol 489:255–274.

Boly M, Moran R, Murphy M, Boveroux P, Bruno MA, Noirhomme Q, et al. 2012. Connectivity changes underlying spectral EEG changes during propofol-induced loss of consciousness. J Neurosci 32:7082–7090.

Boly M, Sanders RD, Mashour G, Laureys S. 2013. Consciousness and responsiveness: lessons from anaesthesia and the vegetative state. Curr Opin Anaesthesiol 26:444–449.

Bonhomme V, Boveroux P, Brichant JF, Laureys S, Boly M. 2012. Neural correlates of consciousness during general anesthesia using functional magnetic resonance imaging (fMRI). Arch Ital Biol 150:155–163.

Bonhomme V, Boveroux P, Hans P, Brichant JF, Vanhaudenhuyse A, Boly M, et al. 2011. Influence of anesthesia on cerebral blood flow, cerebral metabolic rate, and brain functional connectivity. Curr Opin Anaesthesiol 24:474–479.

Boveroux P, Vanhaudenhuyse A, Bruno MA, Noirhomme Q, Lauwick S, Luxen A, et al. 2010. Breakdown of within- and between-network resting state functional magnetic resonance imaging connectivity during propofol-induced loss of consciousness. Anesthesiology 113:1038–1053.

Britz J, Van De Ville D, Michel CM. 2010. BOLD correlates of EEG topography reveal rapid resting-state network dynamics. Neuroimage 52:1162–1170.

Brown EN, Lydic R, Schiff ND. 2010. General anesthesia, sleep, and coma. N Engl J Med 363:2638–2650.

Casali AG, Gosseries O, Rosanova M, Boly M, Sarasso S, Casali KR, et al. 2013. A theoretically based index of consciousness independent of sensory processing and behavior. Sci Transl Med 5:198ra105.

Chalmers DJ. 1998. The problems of consciousness. Adv Neurol 77:7–16; discussion 16–18.

Chang C, Glover GH. 2010. Time-frequency dynamics of resting-state brain connectivity measured with fMRI. Neuroimage 50:81–98.

Cribben I, Wager TD, Lindquist MA. 2013. Detecting functional connectivity change points for single-subject fMRI data. Front Comput Neurosci 7:143.

Crick F, Koch C. 1998. Consciousness and neuroscience. Cereb Cortex 8:97–107.

Devor M, Zalkind V. 2001. Reversible analgesia, atonia, and loss of consciousness on bilateral intracerebral microinjection of pentobarbital. Pain 94:101–112.

Di X, Biswal BB. 2013. Dynamic brain functional connectivity modulated by resting-state networks. Brain Struct Funct [Epub ahead of print] DOI: 10.1007/s00429-013-0634-3.

Edelman GM, Gally JA, Baars BJ. 2011. Biology of consciousness. Front Psychol 2:4.

Ferrarelli F, Massimini M, Sarasso S, Casali A, Riedner BA, Angelini G, et al. 2010. Breakdown in cortical effective connectivity during midazolam-induced loss of consciousness. Proc Natl Acad Sci U S A 107:2681–2686.

Fiset P, Plourde G, Backman SB. 2005. Brain imaging in research on anesthetic mechanisms: studies with propofol. Prog Brain Res 150:245–250.

Franceschini MA, Radhakrishnan H, Thakur K, Wu W, Ruvinskaya S, Carp S, et al. 2010. The effect of different anesthetics on neurovascular coupling. Neuroimage 51:1367–1377.

Franks NP. 2008. General anaesthesia: from molecular targets to neuronal pathways of sleep and arousal. Nat Rev Neurosci 9:370–386.

Franks NP, Zecharia AY. 2011. Sleep and general anesthesia. Can J Anaesth 58:139–148.

Glerean E, Salmi J, Lahnakoski JM, Jaaskelainen IP, Sams M. 2012. Functional magnetic resonance imaging phase synchronization

as a measure of dynamic functional connectivity. Brain Connect 2:91–101.

Gomez F, Phillips C, Soddu A, Boly M, Boveroux P, Vanhaudenhuyse A, et al. 2013. Changes in effective connectivity by propofol sedation. PLoS One 8:e71370.

Greicius MD, Kiviniemi V, Tervonen O, Vainionpaa V, Alahuhta S, Reiss AL, et al. 2008. Persistent default-mode network connectivity during light sedation. Hum Brain Mapp 29:839–847.

Guldenmund P, Demertzi A, Boveroux P, Boly M, Vanhaudenhuyse A, Bruno MA, et al. 2013. Thalamus, brainstem and salience network connectivity changes during propofol-induced sedation and unconsciousness. Brain Connect 3: 273–285.

Gusnard DA, Akbudak E, Shulman GL, Raichle ME. 2001. Medial prefrontal cortex and self-referential mental activity: relation to a default mode of brain function. Proc Natl Acad Sci U S A 98:4259–4264.

Handwerker DA, Roopchansingh V, Gonzalez-Castillo J, Bandettini PA. 2012. Periodic changes in fMRI connectivity. Neuroimage 63:1712–1719.

Hentschke H, Schwarz C, Antkowiak B. 2005. Neocortex is the major target of sedative concentrations of volatile anaesthetics: strong depression of firing rates and increase of GABAA receptor-mediated inhibition. Eur J Neurosci 21:93–102.

Hudetz AG. 2006. Suppressing Consciousness: mechanisms of general anesthesia. Semin Anesth Perioper Med Pain 25: 196–204.

Hudetz AG. 2008. Are we unconscious during general anesthesia? Int Anesthesiol Clin 46:25–42.

Hudetz AG. 2012. General anesthesia and human brain connectivity. Brain Connect 2:291–302.

Hudetz AG, Roman RJ, Harder DR. 1992. Spontaneous flow oscillations in the cerebral cortex during acute changes in mean arterial pressure. J Cereb Blood Flow Metab 12:491–499.

Hudetz AG, Smith JJ, Lee JG, Bosnjak ZJ, Kampine JP. 1995. Modification of cerebral laser-Doppler flow oscillations by halothane, PCO2, and nitric oxide synthase blockade. Am J Physiol 269:H114–H120.

Hutchison RM, Mirsattari SM, Jones CK, Gati JS, Leung LS. 2010. Functional networks in the anesthetized rat brain revealed by independent component analysis of resting-state FMRI. J Neurophysiol 103:3398–3406.

Hutchison RM, Womelsdorf T, Allen EA, Bandettini PA, Calhoun VD, Corbetta M, et al. 2013a. Dynamic functional connectivity: promise, issues, and interpretations. Neuroimage 80:360–378.

Hutchison RM, Womelsdorf T, Gati JS, Everling S, Menon RS. 2013b. Resting-state networks show dynamic functional connectivity in awake humans and anesthetized macaques. Hum Brain Mapp 34:2154–2177.

Jenkinson M, Bannister P, Brady M, Smith S. 2002. Improved optimization for the robust and accurate linear registration and motion correction of brain images. Neuroimage 17: 825–841.

John ER. 2001. A field theory of consciousness. Conscious Cogn 10:184–213.

Jones DT, Vemuri P, Murphy MC, Gunter JL, Senjem ML, Machulda MM, et al. 2012. Non-stationarity in the ''resting brain's'' modular architecture. PLoS One 7:e39731.

Jugovac I, Imas O, Hudetz AG. 2006. Supraspinal anesthesia: behavioral and electroencephalographic effects of intracerebroventricularly infused pentobarbital, propofol, fentanyl, and midazolam. Anesthesiology 105:764–778.

Kalthoff D, Seehafer JU, Po C, Wiedermann D, Hoehn M. 2011. Functional connectivity in the rat at 11.7T: impact of physiological noise in resting state fMRI. Neuroimage 54:2828–2839.

Kang J, Wang L, Yan C, Wang J, Liang X, He Y. 2011. Characterizing dynamic functional connectivity in the resting brain using variable parameter regression and Kalman filtering approaches. Neuroimage 56:1222–1234.

Kannurpatti SS, Biswal BB, Hudetz AG. 2003a. Baseline physiological state and the fMRI-BOLD signal response to apnea in anesthetized rats. NMR Biomed 16:261–268.

Kannurpatti SS, Biswal BB, Hudetz AG. 2003b. Regional dynamics of the fMRI-BOLD signal response to hypoxia-hypercapnia in the rat brain. J Magn Reson Imaging 17:641–647.

Keilholz SD, Magnuson ME, Pan WJ, Willis M, Thompson GJ. 2013. Dynamic properties of functional connectivity in the rodent. Brain Connect 3:31–40.

Kiviniemi V, Vire T, Remes J, Elseoud A, Starck T, Tervonen O, et al. 2011. A sliding time-window ICA reveals spatial variability of the default mode network in time. Brain Connect 1:339–347.

Kiviniemi VJ, Haanpaa H, Kantola JH, Jauhiainen J, Vainionpaa V, Alahuhta S, et al. 2005. Midazolam sedation increases fluctuation and synchrony of the resting brain BOLD signal. Magn Reson Imaging 23:531–537.

Ku SW, Lee U, Noh GJ, Jun IG, Mashour GA. 2011. Preferential inhibition of frontal-to-parietal feedback connectivity is a neurophysiologic correlate of general anesthesia in surgical patients. PLoS One 6:e25155.

Langsjo JW, Alkire MT, Kaskinoro K, Hayama H, Maksimow A, Kaisti KK, et al. 2012. Returning from oblivion: imaging the neural core of consciousness. J Neurosci 32:4935–4943.

Lee U, Kim S, Noh GJ, Choi BM, Hwang E, Mashour GA. 2009a. The directionality and functional organization of frontoparietal connectivity during consciousness and anesthesia in humans. Conscious Cogn 18:1069–1078.

Lee U, Ku S, Noh G, Baek S, Choi B, Mashour GA. 2013. Disruption of frontal-parietal communication by ketamine, propofol, and sevoflurane. Anesthesiology 118:1264–1275.

Lee U, Mashour GA, Kim S, Noh GJ, Choi BM. 2009b. Propofol induction reduces the capacity for neural information integration: implications for the mechanism of consciousness and general anesthesia. Conscious Cogn 18:56–64.

Lewis LD, Weiner VS, Mukamel EA, Donoghue JA, Eskandar EN, Madsen JR, et al. 2012. Rapid fragmentation of neuronal networks at the onset of propofol-induced unconsciousness. Proc Natl Acad Sci U S A 109:E3377–E3386.

Liang Z, King J, Zhang N. 2011. Uncovering intrinsic connectional architecture of functional networks in awake rat brain. J Neurosci 31:3776–3783.

Liu D, Yan C, Ren J, Yao L, Kiviniemi VJ, Zang Y. 2010. Using coherence to measure regional homogeneity of resting-state FMRI signal. Front Syst Neurosci 4:24.

Liu JV, Hirano Y, Nascimento GC, Stefanovic B, Leopold DA, Silva AC. 2013a. fMRI in the awake marmoset: Somatosensory-evoked responses, functional connectivity, and comparison with propofol anesthesia. Neuroimage 78: 186–195.

Liu X, Chang C, Duyn JH. 2013b. Decomposition of spontaneous brain activity into distinct fMRI co-activation patterns. Front Syst Neurosci 7:101.

Liu X, Duyn JH. 2013. Time-varying functional network information extracted from brief instances of spontaneous brain activity. Proc Natl Acad Sci U S A 110:4392–4397.

Liu X, Lauer KK, Ward BD, Li SJ, Hudetz AG. 2013c. Differential effects of deep sedation with propofol on the specific and nonspecific thalamocortical systems: a functional magnetic resonance imaging study. Anesthesiology 118:59–69.

Liu X, Lauer KK, Ward BD, Rao SM, Li SJ, Hudetz AG. 2012. Propofol disrupts functional interactions between sensory and high-order processing of auditory verbal memory. Hum Brain Mapp 33:2487–2498.

Liu X, Pillay S, Li R, Vizuete JA, Pechman KR, Schmainda KM, et al. 2013d. Multiphasic modification of intrinsic functional connectivity of the rat brain during increasing levels of propofol. Neuroimage 83C:581–592.

Liu X, Zhu XH, Zhang Y, Chen W. 2011. Neural origin of spontaneous hemodynamic fluctuations in rats under burst-suppression anesthesia condition. Cereb Cortex 21:374–384.

Lu H, Zou Q, Gu H, Raichle ME, Stein EA, Yang Y. 2012. Rat brains also have a default mode network. Proc Natl Acad Sci U S A 109:3979–3984.

Magnuson M, Majeed W, Keilholz SD. 2010. Functional connectivity in blood oxygenation level-dependent and cerebral blood volume-weighted resting state functional magnetic resonance imaging in the rat brain. J Magn Reson Imaging 32:584–592.

Majeed W, Magnuson M, Keilholz SD. 2009. Spatiotemporal dynamics of low frequency fluctuations in BOLD fMRI of the rat. J Magn Reson Imaging 30:384–393.

Masamoto K, Kanno I. 2012. Anesthesia and the quantitative evaluation of neurovascular coupling. J Cereb Blood Flow Metab 32:1233–1247.

Mashour GA, Alkire MT. 2013. Evolution of consciousness: phylogeny, ontogeny, and emergence from general anesthesia. Proc Natl Acad Sci U S A 110 Suppl 2:10357–10364.

Mason MF, Norton MI, Van Horn JD, Wegner DM, Grafton ST, Macrae CN. 2007. Wandering minds: the default network and stimulus-independent thought. Science 315:393–395.

Mhuircheartaigh RN, Rosenorn-Lanng D, Wise R, Jbabdi S, Rogers R, Tracey I. 2010. Cortical and subcortical connectivity changes during decreasing levels of consciousness in humans: a functional magnetic resonance imaging study using propofol. J Neurosci 30:9095–9102.

Nallasamy N, Tsao DY. 2011. Functional connectivity in the brain: effects of anesthesia. Neuroscientist 17:94–106.

Nasrallah FA, Tan J, Chuang KH. 2012. Pharmacological modulation of functional connectivity: alpha2-adrenergic receptor agonist alters synchrony but not neural activation. Neuroimage 60:436–446.

Pawela CP, Biswal BB, Cho YR, Kao DS, Li R, Jones SR, et al. 2008. Resting-state functional connectivity of the rat brain. Magn Reson Med 59:1021–1029.

Paxinos G, Watson C. 2007. *The Rat Brain in Stereotaxic Coordinates*. San Diego: Academic Press.

Peltier SJ, Kerssens C, Hamann SB, Sebel PS, Byas-Smith M, Hu X. 2005. Functional connectivity changes with concentration of sevoflurane anesthesia. Neuroreport 16:285–288.

Raichle ME, MacLeod AM, Snyder AZ, Powers WJ, Gusnard DA, Shulman GL. 2001. A default mode of brain function. Proc Natl Acad Sci U S A 98:676–682.

Sakoglu U, Pearlson GD, Kiehl KA, Wang YM, Michael AM, Calhoun VD. 2010. A method for evaluating dynamic functional network connectivity and task-modulation: application to schizophrenia. MAGMA 23:351–366.

Sanders RD, Tononi G, Laureys S, Sleigh JW. 2012. Unresponsiveness not equal unconsciousness. Anesthesiology 116: 946–959.

Schrouff J, Perlbarg V, Boly M, Marrelec G, Boveroux P, Vanhaudenhuyse A, et al. 2011. Brain functional integration decreases during propofol-induced loss of consciousness. Neuroimage 57:198–205.

Seth AK, Baars BJ, Edelman DB. 2005. Criteria for consciousness in humans and other mammals. Conscious Cogn 14:119–139.

Seth AK, Izhikevich E, Reeke GN, Edelman GM. 2006. Theories and measures of consciousness: an extended framework. Proc Natl Acad Sci U S A 103:10799–10804.

Smith SM, Miller KL, Moeller S, Xu J, Auerbach EJ, Woolrich MW, et al. 2012. Temporally-independent functional modes of spontaneous brain activity. Proc Natl Acad Sci U S A 109:3131–3136.

Soddu A, Vanhaudenhuyse A, Bahri MA, Bruno MA, Boly M, Demertzi A, et al. 2012. Identifying the default-mode component in spatial IC analyses of patients with disorders of consciousness. Hum Brain Mapp 33:778–796.

Steyn-Ross ML, Steyn-Ross DA, Sleigh JW. 2004. Modelling general anaesthesia as a first-order phase transition in the cortex. Prog Biophys Mol Biol 85:369–385.

Sukhotinsky I, Zalkind V, Lu J, Hopkins DA, Saper CB, Devor M. 2007. Neural pathways associated with loss of consciousness caused by intracerebral microinjection of GABA A-active anesthetics. Eur J Neurosci 25:1417–1436.

Tagliazucchi E, Balenzuela P, Fraiman D, Chialvo DR. 2012a. Criticality in large-scale brain FMRI dynamics unveiled by a novel point process analysis. Front Physiol 3:15.

Tagliazucchi E, Balenzuela P, Fraiman D, Montoya P, Chialvo DR. 2011. Spontaneous BOLD event triggered averages for estimating functional connectivity at resting state. Neurosci Lett 488:158–163.

Tagliazucchi E, von Wegner F, Morzelewski A, Brodbeck V, Laufs H. 2012b. Dynamic BOLD functional connectivity in humans and its electrophysiological correlates. Front Hum Neurosci 6:339.

Tononi G. 2004. An information integration theory of consciousness. BMC Neurosci 5:42.

Tononi G. 2012. Integrated information theory of consciousness: an updated account. Arch Ital Biol 150:293–329.

Tononi G, Koch C. 2008. The neural correlates of consciousness: an update. Ann N Y Acad Sci 1124:239–261.

Tu Y, Yu T, Fu XY, Xie P, Lu S, Huang XQ, et al. 2011. Altered thalamocortical functional connectivity by propofol anesthesia in rats. Pharmacology 88:322–326.

Upadhyay J, Baker SJ, Chandran P, Miller L, Lee Y, Marek GJ, et al. 2011. Default-mode-like network activation in awake rodents. PLoS One 6:e27839.

Velly LJ, Rey MF, Bruder NJ, Gouvitsos FA, Witjas T, Regis JM, et al. 2007. Differential dynamic of action on cortical and subcortical structures of anesthetic agents during induction of anesthesia. Anesthesiology 107:202–212.

Veselis RA. 2001. Anesthesia—a descent or a jump into the depths? Conscious Cogn 10:230–235; discussion 246–258.

Vincent JL, Patel GH, Fox MD, Snyder AZ, Baker JT, Van Essen DC, et al. 2007. Intrinsic functional architecture in the anaesthetized monkey brain. Nature 447:83–86.

Wang K, van Meer MP, van der Marel K, van der Toorn A, Xu L, Liu Y, et al. 2011. Temporal scaling properties and spatial synchronization of spontaneous blood oxygenation level-dependent (BOLD) signal fluctuations in rat sensorimotor network at different levels of isoflurane anesthesia. NMR Biomed 24:61–67.

White NS, Alkire MT. 2003. Impaired thalamocortical connectivity in humans during general-anesthetic-induced unconsciousness. Neuroimage 19:402–411.

Williams KA, Magnuson M, Majeed W, LaConte SM, Peltier SJ, Hu X, et al. 2010. Comparison of alpha-chloralose, medetomidine and isoflurane anesthesia for functional connectivity mapping in the rat. Magn Reson Imaging 28:995–1003.

Zang Y, Jiang T, Lu Y, He Y, Tian L. 2004. Regional homogeneity approach to fMRI data analysis. Neuroimage 22:394–400.

Zecharia AY, Franks NP. 2009. General anesthesia and ascending arousal pathways. Anesthesiology 111:695–696.

Zhang N, Rane P, Huang W, Liang Z, Kennedy D, Frazier JA, et al. 2010. Mapping resting-state brain networks in conscious animals. J Neurosci Methods 189:186–196.

Zhao F, Zhao T, Zhou L, Wu Q, Hu X. 2008. BOLD study of stimulation-induced neural activity and resting-state connectivity in medetomidine-sedated rat. Neuroimage 39: 248–260.

Address correspondence to:
Anthony G. Hudetz
Department of Anesthesiology
Medical College of Wisconsin
8701 Watertown Plank Road
Milwaukee, WI 53226

E-mail: ahudetz@mcw.edu